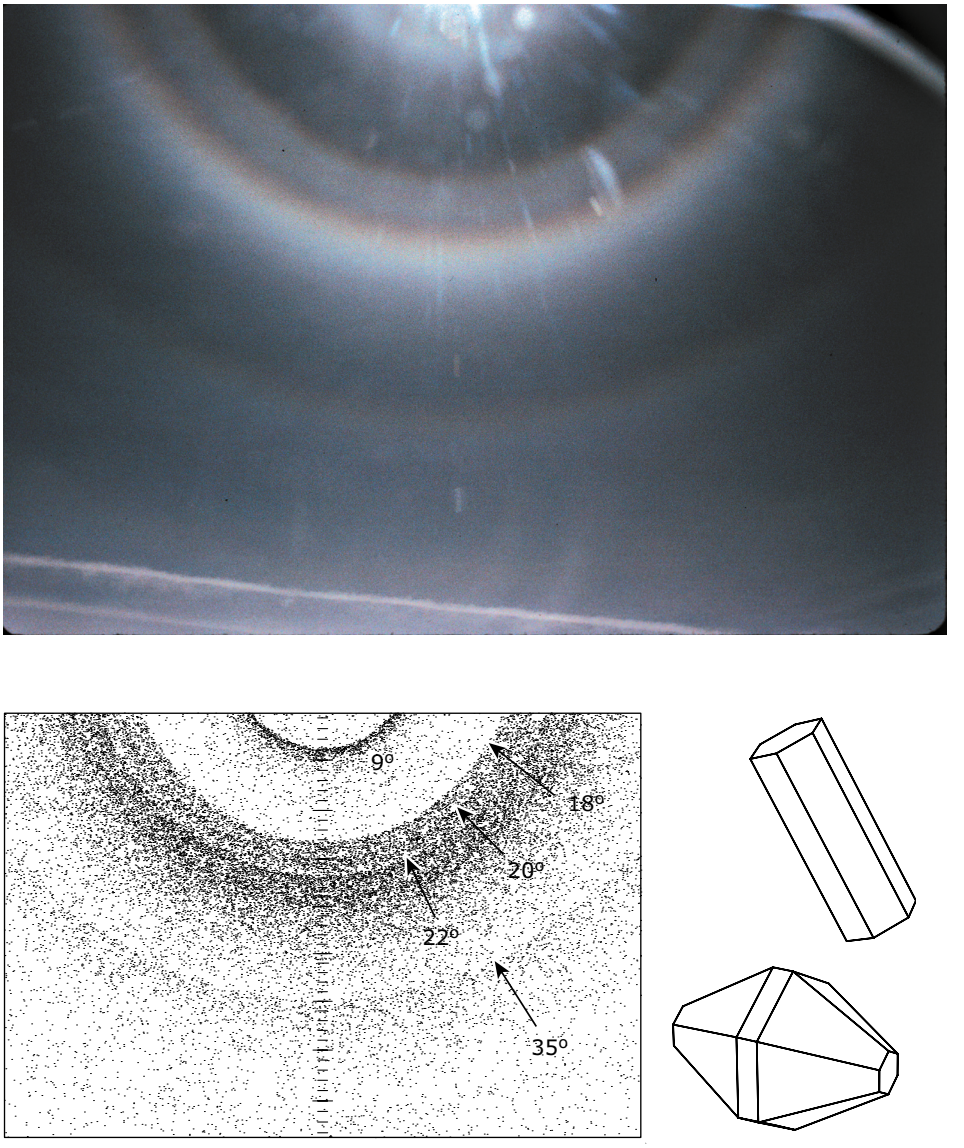

FIGURE 8.1 Odd radius circular halos seen from an airplane at 31,000 feet over British Columbia. In the photograph the 18°, 22° (or 23°?), and 35° halos are colorful and easy to see. Between the 18° and 22° halos the 20° halo is faint but unusually sharp and distinct. The 23° and 24° halos are probably present but masked by the bright 22° halo. The 9° halo is bright but nearly lost in the glare at the top of the airplane window. The simulation of the display was made using randomly oriented crystals shaped like those shown. The pyramidal crystals made the odd radius halos in the simulation, and the prismatic crystals made the 22° halo. The pyramid faces of the crystals are the $\{10\bar{1}1\}$ faces, the simplest crystallographically possible pyramid faces. Tick marks in the simulation are at intervals of one degree.

CHAPTER 8

Odd Radius Circular Halos

The halo display in Figure 8.1 was seen from a commercial jet flying over British Columbia between Seattle and Anchorage in 1999. The display consists of several odd radius circular halos and in fact is probably almost identical to the display seen by Weickmann nearly six decades earlier (Chapter 1). The simulation in the figure shows the circular halos that would be theoretically expected from randomly oriented prismatic and pyramidal crystals as shown. The pyramid faces of the crystals are the $\{1\,0\,\bar{1}\,1\}$ faces, which, as mentioned in Chapter 7, are the simplest theoretically possible pyramid faces. The pyramidal crystals here can therefore be regarded as the next logical step in complexity after the simple prismatic crystals of Chapters 1–6. Using the same ideas that guided Steinmetz and Weickmann (Chapter 7), we will see that crystals like these should theoretically be able to make as many as eight circular halos, having radii of about 9°, 18°, 20°, 22°, 23°, 24°, 35°, and 46°. The radii of the halos in the photograph are difficult to measure accurately, but they appear to be at least roughly consistent with the theoretically expected values. (Although only five halos are seen distinctly in this particular photograph, the 22°, 23°, and 24° halos are probably overlapping to give the appearance of a single halo. The 46° halo, though seen only faintly here, is stronger in other photographs of the display.) These eight halos are by far the most common of the circular halos; any other circular halo would be considered highly exotic.

The circular halos arise in (more or less) randomly oriented crystals. Their ray paths enter and directly exit the crystal, with internal reflections playing no essential role. Each circular halo is associated with such a ray path or, equivalently, with a *wedge angle,* the wedge angle being the angle between the entry and exit faces of the ray path. Table 8.1 gives the wedge angles and theoretical halo radii

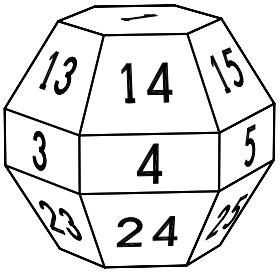

FIGURE 8.2 Face numbering on a pyramidal crystal. The basal faces are numbered 1 and 2, and the prism faces are 3, 4, . . . , 8, the same as for prismatic crystals. The pyramid faces are 13, 14, . . . , 18, and 23, 24, . . . , 28. The pyramid faces here are the $\{10\bar{1}1\}$ faces, but the numbering scheme is standard for any pyramidal crystal.

for the eight circular halos mentioned above.

How do the theoretical halo radii in the table square with the radii of real halos? The British Columbia display is not a good test, because, as already mentioned, the halo radii in the photo are hard to measure. Not only is the sun out of the photo, there is also the complication of distortion introduced by the airplane window.

The display shown in Figures 8.3 and 8.4 has fewer halos, but it is a very strong display nevertheless. Using the methods of Appendix D, we have positioned orange, blue, and red dots in the photo at respective angular distances of 18.3°, 22.9°, and 34.9° from the sun; these are the theoretical radii of the 18°, 23°, and 35° halos (Table 8.1). The orange, blue, and red dots do indeed end up on the inner edges of three circular halos; apparently the halos are the 18°, 23°, and 35° halos. The 20° halo may be present as well, blending with the 18° halo. But although ordinary 22° parhelia are prominent, there is no 22° halo. That is, there is no circular halo at the green dots, which are 21.8° from the sun, where the 22° halo would be

TABLE 8.1 Wedges (or ray paths), wedge angles, and theoretical halo radii of circular halos made by ice crystals having basal, prism, and $\{10\bar{1}1\}$ pyramid faces (Figure 8.2).

Wedge	Wedge angle α	Halo radius Δ_{min}	Halo name
13 6	28.0°	8.9°	9° halo
13 25	52.4	18.3	18° halo
13 16	56.0	19.9	20° halo
3 5	60.0	21.8	22° halo
13 2	62.0	22.9	23° halo
13 5	63.8	23.8	24° halo
13 15	80.2	34.9	35° halo
1 3	90.0	45.7	46° halo

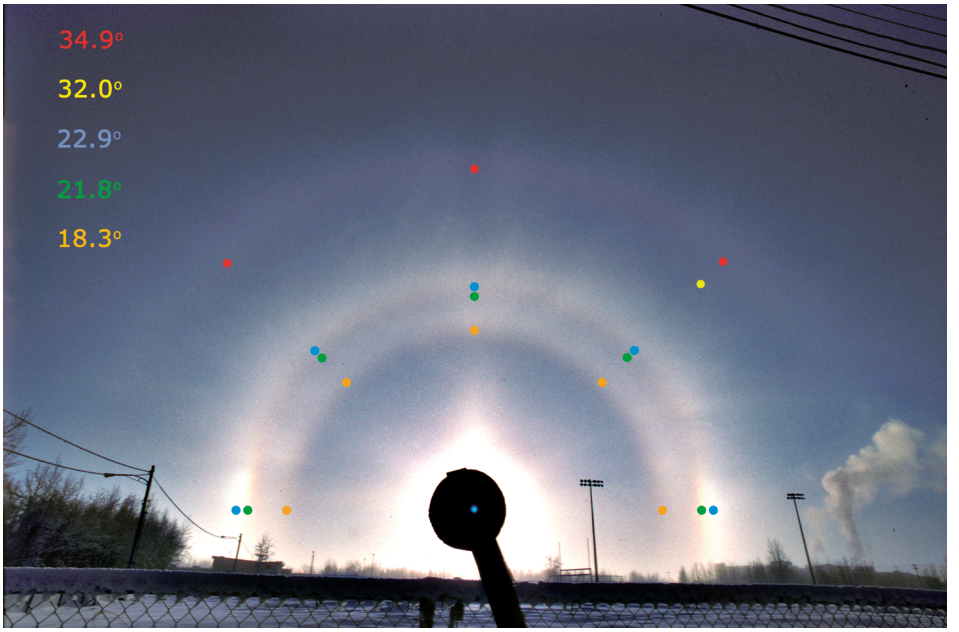

FIGURE 8.3 The 18°, 23°, and 35° halos. Ordinary 22° parhelia are present as well, at left and right, clearly closer to the sun than is the 23° halo. The colored dots are at the indicated angular distances from the sun. The sun, barely more than a grey dot here, is seen through a nearly opaque disk made from crossed polarizers. Fairbanks, January 31, 2005.

FIGURE 8.4 Slightly later stage of the same display, photographed with a wider angle lens and different film.

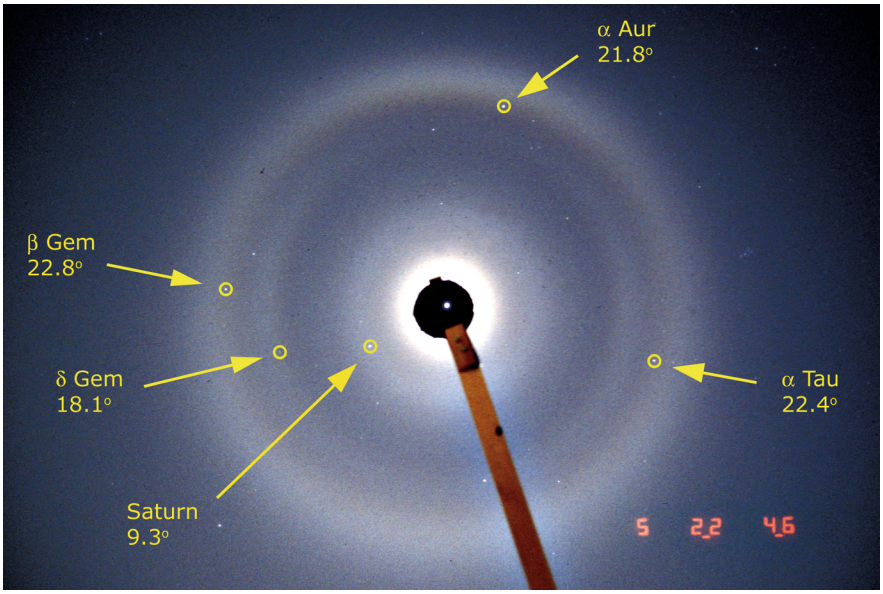

FIGURE 8.5 Odd radius lunar halos. The indicated angular distances from the moon to the circled stars can be used to estimate the halo radii. The most prominent halos appear to be the 9°, 18°, and 23° halos. Fairbanks, Alaska, January 5, 2004, 10:46 P.M. Moon elevation 50°.

expected to be. The significance of the yellow dot, at the 1:30 position and 32° from the sun, will be explained in Chapter 11, in connection with Figure 11.4.

Positioning the colored dots at prescribed angular distances from the sun is more involved than it may sound, and measuring the radii of daytime halos from a photograph is always a tricky business. But a photograph of lunar halos is another matter. If the photo contains some stars, then accurate angular distances from the moon to the various stars are easily computed, so long as the time and place of the photo are known.

Thus, in Figure 8.5 the angular distances from the circled stars to the moon are known quite accurately—to better than .05°. The positions of the circled stars relative to the moon and the halos are just what you would expect from Table 8.1 if the halos in the photo are the 9°, 18°, and 23° circular halos: The position of Saturn, 9.3° from the moon and about at the inner edge of the inner halo, is just right if the halo is the 9° halo (theoretical radius 8.9°). The position of the star δ Gem at 18.1° from the moon and at the inner edge of the intermediate halo, is correct if the halo is the 18° halo (theoretical radius 18.3°). The positions of the three outer stars suggest that the outer halo is the 23° halo rather than the common 22° halo; the halo is just a bit too far from the moon to be the 22° halo.

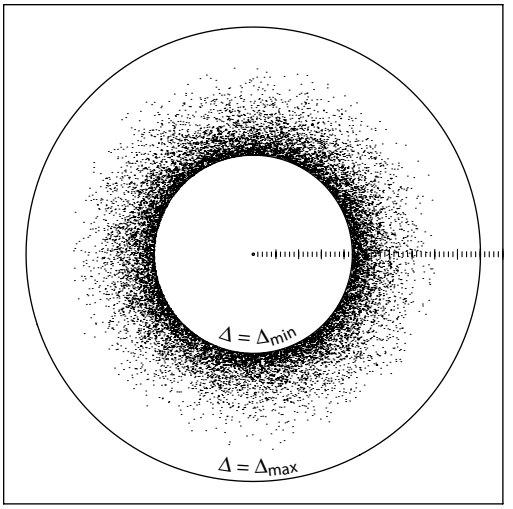

FIGURE 8.6 Idealized simulation of the 22° halo. The crystals used in making the simulation were randomly oriented hexagonal prisms. Only ray paths 35 were allowed, so that, for example, there were no reflected rays and no 46° halo rays. The two circles are the theoretical inner and outer boundaries of the halo, on which $\Delta = \Delta_{min}$ and $\Delta = \Delta_{max}$. The sun was a point sun, and the light rays were all of one wavelength; as a result, the inner edge of the halo appears unrealistically sharp.

In the next chapter we will see how the wedge angles in Table 8.1 were calculated. In doing so, we will also begin to see in what sense the $\{10\bar{1}1\}$ faces are simple. In the next two sections of the present chapter we will see how the halo radii in Table 8.1 were calculated from the wedge angles. We begin by examining the 22° halo; it will serve as a prototype for all circular halos.

The 22° halo as a prototype for all circular halos

The 22° halo normally arises in prismatic crystals, but it can also arise in pyramidal crystals like the one in Figure 8.2, since that crystal has the necessary prism faces. The crystals should be randomly oriented and the ray path should be 35 (or 46, 57, etc.), so that the wedge angle is 60°. As a crystal takes on all orientations, the halo point—the light point of the outgoing ray—traces out the halo. Since all orientations are allowed, you might think that the halo point would trace out the entire celestial sphere, but in fact the angular deviation Δ between the sun and the halo point ranges not from 0° to 180° but only from $\Delta_{\min} = 21.8°$ to $\Delta_{\max} = 50.1°$, and the halo point traces out an annular region on the celestial sphere (Figure 8.6). The portion of the halo near the outer boundary $\Delta = \Delta_{\max}$ is far too weak to be seen, and normally what you notice in the sky is mainly the relatively abrupt change in brightness at the inner boundary $\Delta = \Delta_{\min}$. In fact we often carelessly refer to the inner boundary as the 22° halo, thus treating the halo as a circle rather than as an annular region.

Figure 8.7 illustrates the wedge angle for the 22° halo. The figure also attempts to illustrate the idealized wedge that is the source of the term wedge angle. The wedge is bounded by planar extensions of faces 3 and 5 and extends indefinitely

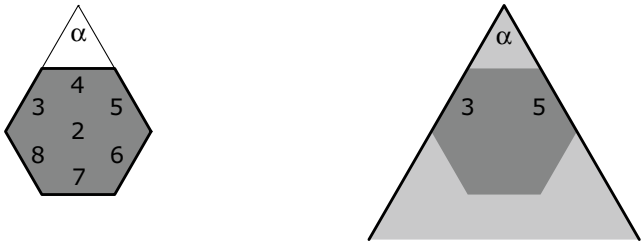

FIGURE 8.7 (*Left*) Wedge angle $\alpha = 60°$ for the wedge 35 on a crystal as in Figure 6.1 or Figure 8.2. This wedge gives the 22° halo. (*Right*) Wedge 35. The wedge is determined by faces 3 and 5 of the crystal. The hexagon represents the crystal, and the large triangle enclosing the hexagon represents the wedge. The view is looking directly at face 2 of the crystal.

in both directions perpendicular to the page, and indefinitely in the direction toward the bottom of the page as well, so that there are only two faces bounding the wedge. We sometimes imagine for simplicity that the 22° halo arises in wedges like this one.

Halo radii from wedge angles

Other circular halos are like the 22° halo but with different wedge angles α. Both $\Delta_{\min}$ and $\Delta_{\max}$ depend on α and, hence, so does the annular region occupied by the halo. The parameter $\Delta_{\max}$ is usually unimportant, since the halo is so weak near its outer boundary, but $\Delta_{\min}$ is crucial—it is the halo radius. In the next section we will derive the classical expression for the dependence of $\Delta_{\min}$ on α, namely,

$$\sin \frac{\alpha + \Delta_{\min}}{2} = n \sin \frac{\alpha}{2} \tag{8.1}$$

where $n = 1.31$ is the refractive index for ice. For the 22° halo, the wedge angle α is 60° and so $\Delta_{\min}$ is 21.8°. For the 46° halo, the wedge angle is 90° and $\Delta_{\min}$ is 45.7°. The other halo radii $\Delta_{\min}$ in Table 8.1 are calculated similarly, once their wedge angles are known.

In general, larger wedge angles give larger halo radii. However, there is a largest wedge angle $\alpha_{\max}$ that will allow light to pass through the wedge. For a wedge with $\alpha > \alpha_{\max}$, any light ray that enters the wedge at one face suffers total internal reflection at the other. We will see that $\alpha_{\max}$ is given by

$$n \sin \frac{\alpha_{\max}}{2} = 1 \tag{8.2}$$

For ice, with $n = 1.31$, Eq. (8.2) gives $\alpha_{\max} = 99.5°$. Equation (8.1) then gives a largest possible halo radius of $\Delta_{\min} = 80.5°$, but in practice this value is too generous, and any halo having a radius greater than about 50° would probably be too faint to be seen.

On a hexagonal prism there are three wedge angles, namely, 60°, 90°, and 120°. The wedge angles 60° and 90° make the 22° and 46° halos, but the wedge angle 120° is greater than $\alpha_{\max}$. The 22° and 46° halos are therefore the only circular halos that can arise in hexagonal prisms. To make additional circular halos, you need additional wedge angles and therefore a crystal other than a simple hexagonal prism. A pyramidal crystal is a natural choice, but to specify its shape—and hence the wedge angles—you need to know the angle of inclination between the pyramid faces and the crystal axis, and this is where halo theorists were for a long time in the dark. Had they known this angle, they could have found the wedge angles and then calculated the halo radii using Eq. (8.1), which has long been known. On the other hand, had they known the halo radii with some precision, they could have worked backwards to get the wedge angles and perhaps the crystal shape. But they knew neither, at least not with any certainty.

Today we have many photographs of odd radius halos, and we can measure the halo radii from the photos. The measurements require care, however, and even under the best circumstances the measured radii are uncertain by half a degree or so, the uncertainty being due mainly to the fuzziness of the halo edge. We also have photographs of pyramidal crystals, and we can measure wedge angles from the photos, but again the results are not as precise as we would like. The most precise values for wedge angles are today calculated theoretically from crystallographic principles. In the next chapter we will show how these calculations go.

Topics in the present chapter have been arranged roughly in order of decreasing importance. On a first reading, you may wish to skip directly from here to the next chapter.

How light passes through a wedge

In order to understand circular halos and, in particular, in order to derive Eq. (8.1), we need to think about the way light passes through a wedge. How much is the light deviated? Is there a minimum value for the deviation? Is there a maximum? And so forth. The problem of light passing through a wedge is not so simple, since it is spatial. Veterans of Physics 101 may remember something like it, but usually what is treated there is the special case where the ray path lies entirely in a plane normal to both faces of the wedge. In many books on halos the problem is similarly swept under the rug. The general problem, not just the special case,

has been treated by Uhler [81] and Tape [75], both of whom approached the problem analytically. Our approach here is geometric. You will see the appeal of the geometric approach if you glance at one of the analytic treatments for comparison.

As usual, we consider a light ray passing through a wedge having refractive index n and wedge angle α. Figure 8.8 shows the light points **S**, **R**, and **H** of the entry, internal, and exit rays. The sun point **S** and the halo point **H** are on the sphere of radius 1, while **R** is on the sphere of radius $n > 1$. The law of refraction (page 38) tells how to get **H** from **S**: you project **S** to the outer sphere, getting **R**, and then project **R** back to the inner sphere, getting **H.** The first projection is normal to the entry face, the second is normal to the exit face.

We refer to the V-shaped configuration consisting of the two red line segments **RS** and **RH** as the *vee* or the *normal vee,*[1] since its legs—the two line segments—are the projection directions and hence are normal to their respective wedge faces. As the wedge takes on various orientations, the point **S** in Figure 8.8 stays fixed, but **R** moves on the outer sphere and **H** moves on the inner sphere, always in such a way that the vertex angle of the vee remains equal to the wedge angle α. The halo point **H** traces out the circular halo.

Minimum deviation In Figure 8.8 the deviation between the points **S** and **H** is, in radians, the great circle distance between **S** and **H.** It is closely related to the straight line distance between **S** and **H**; the smaller the deviation, the smaller the straight line distance. It is clear from the figure that you can't make **S** and **H** arbitrarily close together and you can't make them arbitrarily far apart. So you can't make the deviation arbitrarily small and you can't make it arbitrarily big. What are the normal vees for which the deviation is minimum? What are those for which it is maximum?

Figure 8.9 shows how to narrow down the candidates both for minimum and for maximum deviation. If you start with a normal vee that is not isosceles, you can always find a nearby vee which has smaller deviation: In the top diagram, if you start with the vee formed by **S**, **R**, and **H**, you can perturb it to the vee formed by **S′**, **R** and **H′**, always keeping the vertex angle equal to α. Since the segment **RH** was more nearly perpendicular to the inner circle than was **RS**, the perturbation decreases the deviation. (The straight-line distance between **S′** and **H′** is less than that between **S** and **H.**) Continuing this process, you arrive at an isosceles vee (middle diagram) which has smaller deviation than the original vee.

A vee is said to be *central* if the plane of the vee passes through the common

[1] More precisely, points **S**, **R**, and **H** define a *normal vee* (with parameters n and α) if **S** and **H** are on the inner sphere, **R** is on the outer sphere, $\angle\mathbf{SRH} = \alpha$, and the line segments **RS** and **RH** do not penetrate the inner sphere. In this case the corresponding ray path and wedge, including the wedge orientation, can be reconstructed from **S**, **R**, and **H.**

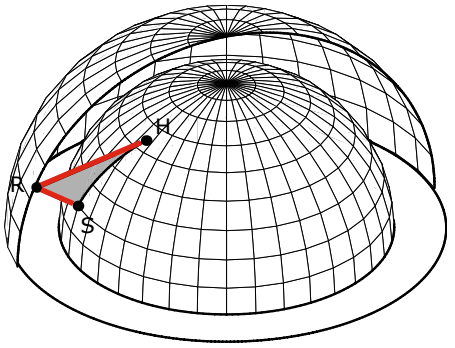

FIGURE 8.8 Light point diagram for the circular halo forming in a wedge having refractive index n and wedge angle α. The spheres are concentric and have radii 1 and n. As the wedge (not shown) changes its orientation, the normal vee (red), consisting of the line segments **RS** and **RH**, changes also; the sun point **S** is fixed on the inner sphere, and the vertex angle of the vee remains equal to α, but the point **R** can move on the outer sphere, and the halo point **H** can move on the inner sphere, where it traces out the halo.

center **O** of the two spheres. Among all the isosceles vees **SRH** with vertex at **R** and with fixed vertex angle α, the ones with smallest deviation are clearly those that are central. After all, the isosceles triangles **SRH** are all similar, and we just want the ones with the shortest side **SH**.

Thus, among all vees associated with the given wedge, the ones that give minimum deviation $\Delta_{\min}$ are those that are isosceles and central. One such vee is shown at the top in Figure 8.10. The Law of Sines applied to the lower left diagram in the figure gives Eq. (8.1), the fundamental equation for finding halo radius in terms of wedge angle.

Historically, any plane that is normal to both faces of the wedge has been known as a *normal plane.* A vee is central when the corresponding ray path lies entirely in a normal plane; this is because the plane of any vee **SRH** is itself a normal plane, and because the entry, internal, and exit rays are in the directions **SO**, **RO**, and **HO**, respectively. A ray path has minimum deviation when it lies in a normal plane and is symmetric (Figure 8.10, lower right).

Maximum deviation Figure 8.9 shows that the maximum deviation $\Delta_{\max}$ can only occur when the vee is tangential, that is, when at least one of its legs is tangent to the sphere. It turns out that, depending on n and α, the maximum occurs either when the vee is tangential and central, or when the vee is tangential and isosceles. For ice, with $n = 1.31$, the former configuration gives the maximum deviation if $\alpha \leq 46.9°$, and the latter gives it if $\alpha \geq 46.9°$. The result is

$$\Delta_{\max} = \begin{cases} -\alpha + \cos^{-1}\left(\cos\alpha - \sqrt{n^2-1}\,\sin\alpha\right) & \text{if } \alpha \leq 46.9° \\ 2\sin^{-1}\left(\sqrt{n^2-1}\,\sin\frac{\alpha}{2}\right) & \text{if } \alpha \geq 46.9° \end{cases} \tag{8.3}$$

For example, the outer boundary of the 22° halo is at $\Delta_{\max} = 50.1°$, since $\alpha = 60° > 46.9°$. For more on both minimum and maximum deviation see the article by Tape [74].

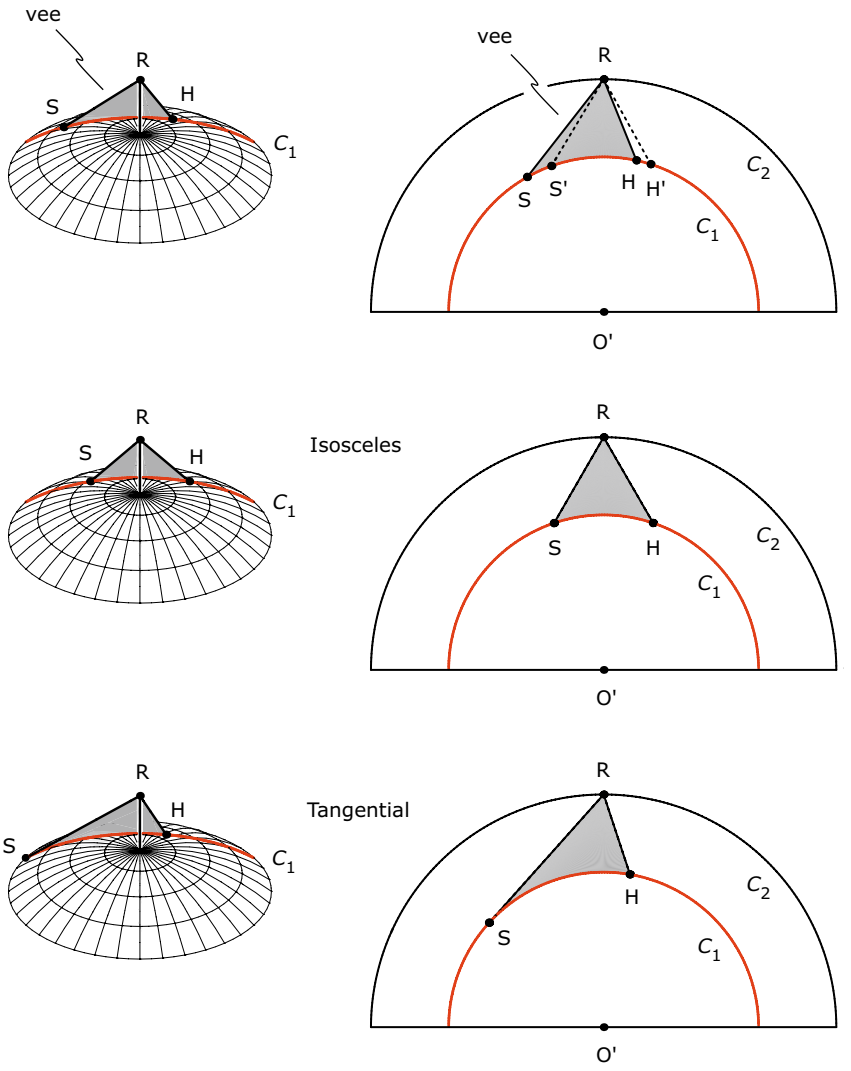

FIGURE 8.9 Several normal vees, all in the same plane, showing that isosceles vees are the only candidates for minimum deviation, and tangential vees are the only candidates for maximum deviation. The situation is similar to that in Figure 8.8 except that here **R** is fixed, rather than **S**. At the left in each diagram the points **S** and **H** are on the sphere of radius 1. The point **R** is on the sphere of radius n (not shown). The plane of the vee intersects the sphere of radius 1 in the circle C_1 (red). At the right is the section in the plane of the vee, with circle C_1 as before and with circle C_2 being the intersection of the plane of the vee with the sphere of radius n. Note that the point O', which is the common center of the two circles, is not the center of the sphere. (*Top*) An arbitrary vee. Also shown is a perturbation of the vee (dashed) having the same vertex angle and lying in the same plane. Perturbing the vee so as to make it more nearly isosceles, as here, decreases the deviation. Perturbing it so as to make it more nearly tangential increases the deviation. (*Middle*) Isosceles vee. (*Bottom*) Tangential vee.

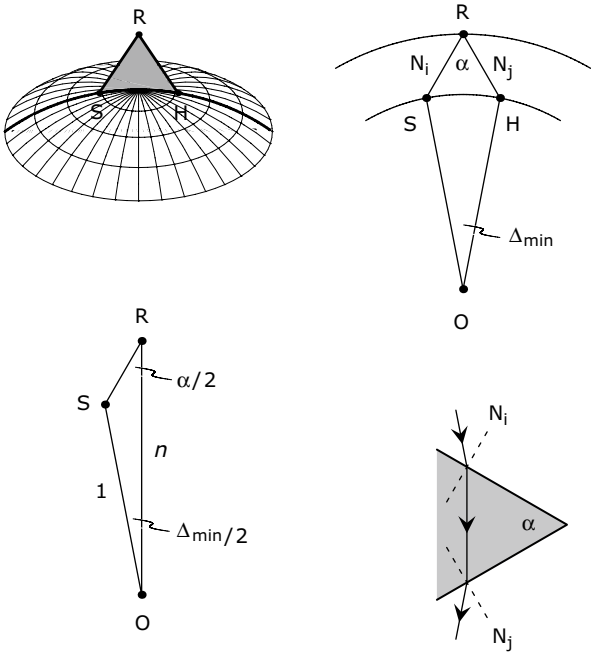

FIGURE 8.10 Calculating the minimum deviation Δ_{min} [Eq. (8.1)]. (*Top left*) Light points **S**, **R**, **H** in minimum deviation configuration. The vee formed by **S**, **R**, and **H** is isosceles and central. (*Top right*) Same but showing only the section in the plane of the vee. Since the vee is central, the plane contains the center **O** of the sphere. (*Bottom left*) The triangle **SRO**, which gives Eq. (8.1) via the Law of Sines. (*Bottom right*) The corresponding wedge and ray path. The entry, internal, and exit rays are in the directions **SO, RO**, and **HO**, respectively. The ray path is symmetric and lies in a plane normal to both faces of the wedge.

Maximum wedge angle The wedge angle is maximum when a central isosceles vee is also tangential. Then $\angle$**OSR** in Figure 8.10 becomes a right angle, giving Eq. (8.2).

Fine tuning the halo radii

One can argue that the theoretical halo radii Δ_{min} in Table 8.1 should be refined. Even if the wedge angles in the table are exactly right—which we assume for the moment—there are many factors that might cause small perturbations in halo radii. Some of the perturbations can be predicted quantitatively, but others are elusive. Let's again consider the 22° halo as an example.

Dependence of halo radius on sun size We have been treating halos as if the light source were a point, but of course the sun has a positive angular diameter—about half a degree. Each point on the sun's disk can be thought of as making its own 22° halo, and what we normally call the 22° halo is really a superposition of all these halos (annular regions). A small subtraction δ from our value $\Delta_{\text{min}} = 21.8°$ (Table 8.1) should therefore be made in computing the radius of the 22° halo. You might think at first that δ should be equal to the angular radius of the sun, but Figure 8.11 suggests that it should be less, perhaps 0.15° or so. (We are just

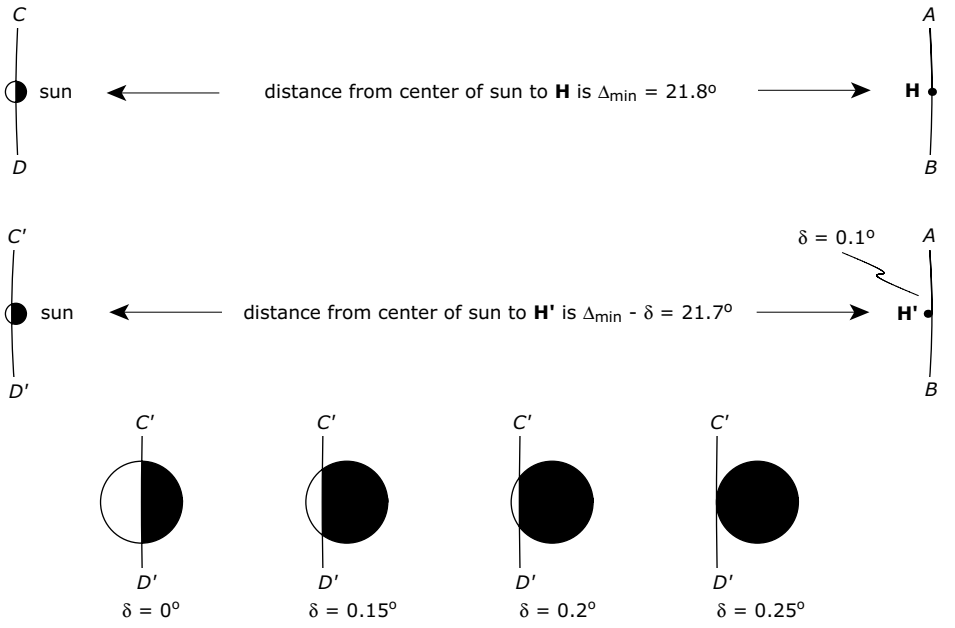

FIGURE 8.11 The effect of the positive angular size of the sun on halo radius. (*Top*) Sun and point **H** at a distance $\Delta_{min} = 21.8°$ (for 22° halo) from the center of the sun. Arc *AB* is part of the circle of radius Δ_{min} centered at the center of the sun. Arc *CD* is part of the circle of radius Δ_{min} centered at **H**. Points on the white part of the sun's disk can light the point **H** via 22° halo ray paths, since they are Δ_{min} or a bit more from **H**. (*Middle*) Same except that **H** has been replaced by **H′** at a distance $\delta = 0.1°$ to the left of **H**, and arc *CD* has been replaced accordingly by arc *C′D′*. Points on the white part of the sun's disk can light **H′**. (*Bottom*) Same but for $\delta = 0°, 0.15°, 0.2°, 0.25°$. With $\delta = 0.2°$ the white fraction of the sun's disk is perhaps too small to be significant. Thus the correction in halo radius due to the positive angular size of the sun should be 0.15° or so.

guessing.) Halo simulations made both with and without a point sun barely differ from each other, thus suggesting that δ might be even less.

Dependence on temperature and pressure It is clear from Eq. (8.1) that $\Delta_{\min}$ depends on the refractive index n of ice as well as on the wedge angle α. But n depends slightly on temperature and pressure, and hence so does $\Delta_{\min}$. A crude approximation for the dependence of n is

$$n(T, P) \approx 1.31 - 3.82 \times 10^{-5}(T + 3) - .035 \times 10^{-5}\, P, \tag{8.4}$$

where $n(T, P)$ is the refractive index of ice in air at temperature T (degrees Celsius) and pressure P (hectopascals). The base value $n = 1.31$, which appears in Eq. (8.4) and which is the value that was used in calculating the $\Delta_{\min}$-values in Table 8.1, is for $T = -3$ and $P = 0$. Using Eqs. (8.1) and (8.4), you can estimate the impact of temperature and pressure changes on halo radius. You will find that

the pressure is negligible but that temperature matters, though barely: the radius of the 22° halo at –55°C is about 0.15° larger than that at –3°C. The temperature here of course refers to the temperature where the ice crystals are located, so –55°C is not unreasonable when the halos are forming in high cloud. For such halos the increase in halo radius due to the low temperature should therefore about balance the decrease due to positive sun size. For a halo display forming at warmer temperatures, say –25°C, the change due to temperature would be less, and the temperature and sun size corrections together would give a net decrease of about 0.1° in the theoretical halo radius—not much.

Dependence on wavelength The refractive index also depends on the wavelength (color) of the light under consideration, and hence so does $\Delta_{\min}$. Both n and $\Delta_{\min}$ are smallest for red light, largest for violet. Thus the 22° halo is a superposition of many concentric circular halos, one for each wavelength, with the red halos being the smallest and the violet halos being the largest. The resulting superposition tends to look reddish on its inner edge; this is where only the red halos are seen, with no overlap from the other colors.

Table 8.2 gives $\Delta_{\min}$ both for red light ($n = 1.307$) and for yellow light ($n = 1.31$). When we speak of "the" value of $\Delta_{\min}$ for a halo, we generally mean $\Delta_{\min}$ for yellow light; this is what was given in Table 8.1. But if you are interested in the red, i.e., innermost, part of a halo, then you should use the slightly smaller $\Delta_{\min}$-value for red light, especially in the case of the larger halos, where the difference between red and yellow becomes substantial.

Are the theoretical halo radii correct? Using the methods of Appendix D, we have positioned the four yellow dots in Figure 8.12 so that their angular distances

TABLE 8.2 Same as Table 8.1 but with halo radii computed for red as well as for yellow light. The 77° halo (bottom line of the table), which in principle exists for red light but not for yellow, would be far too weak to be seen.

Wedge	Wedge angle α	Halo radius Δ_{min} (red, $n = 1.307$)	Halo radius Δ_{min} (yellow, $n = 1.31$)	Halo name
13 6	28.0°	8.9°	8.9°	9° halo
13 25	52.4	18.1	18.3	18° halo
13 16	56.0	19.7	19.9	20° halo
3 5	60.0	21.6	21.8	22° halo
13 2	62.0	22.6	22.9	23° halo
13 5	63.8	23.6	23.8	24° halo
13 15	80.2	34.5	34.9	35° halo
1 3	90.0	45.1	45.7	46° halo
13 24	99.8	76.9	…	77° halo

from the sun are 21.8°; this is the $\Delta_{\min}$-value of the 22° halo for yellow light. The red dots are at 21.6°, the $\Delta_{\min}$-value for red light. The locations of the dots look about right with respect to the halo, with the red dots ending up on the inner edge of the halo and the yellow dots being just a bit farther out. Here no corrections would be expected for sun size and temperature, since the display occurred in high cloud, where the temperature was probably low, so that the two corrections would cancel each other.

Figure 8.13 is another example, the yellow and red dots having the same meaning as before. To our eye the red and yellow dots in the 12:00 position look about right, but the ones at 3:00 and 9:00 look just a hair too close to the sun. (The ones at 6:00 are in an overexposed region and are irrelevant.) Correcting for sun size and temperature would make the discrepancy worse, though ever so slightly. Perhaps we have a bug in our measurement of angular distances, or perhaps we are still forgetting some adjustment to n. (Or perhaps the whole theory is fundamentally flawed, though of course we do not think so.) But it may also be that the 22° halo here is in fact not perfectly circular. It is easy to see how this might happen if the crystals are not required to have completely random orientations.

In any case, if Figures 8.12 and 8.13 are any indication, the $\Delta_{\min}$-values in Table 8.1 need very little refinement, if any. If desired, small corrections can be made for sun size, temperature, and color. But usually we will not do so; when we speak of the theoretical radius of a halo, we generally mean the $\Delta_{\min}$-value from Table 8.1, uncorrected.

The inner edge of a halo is always fuzzy to some extent, which makes it difficult to measure the radius. Because the inner edges of halos are so hard to pinpoint, we have ducked the problem by not attempting to mark them in our photographs. Thus in Figures 8.12, rather than trying to indicate the inner edge of the halo, we have been content to position the red and yellow dots at the angular distances given by the $\Delta_{\min}$-values for red and yellow light. We then leave it to you to decide whether the edge of the halo is consistent with the dot locations.

Three more caveats Although the analyses in Figures 8.12 and 8.13 are reassuring, we have no reason to be complacent. We can think of at least three more factors that complicate the treatment of halo radii: halo brightness, atmospheric refraction, and diffraction.

In Figure 3.7 the bright lower tangent arc is slightly closer to the moon than is the much dimmer 22° halo—an impossibility, according to theory (Figure 12.2). But that theory ignores the role of the eye and the brain, it ignores the role of the camera and all of the attendant issues involving exposures, processing, and possible electronic manipulation of the photo, and it ignores forward scattering of light, the same forward scattering that creates the aureole around the sun and

FIGURE 8.12 Ordinary 22° halo. Yellow dots are 21.8° from the sun, red dots are at 21.6° (Table 8.2). Fairbanks, July 9, 2004.

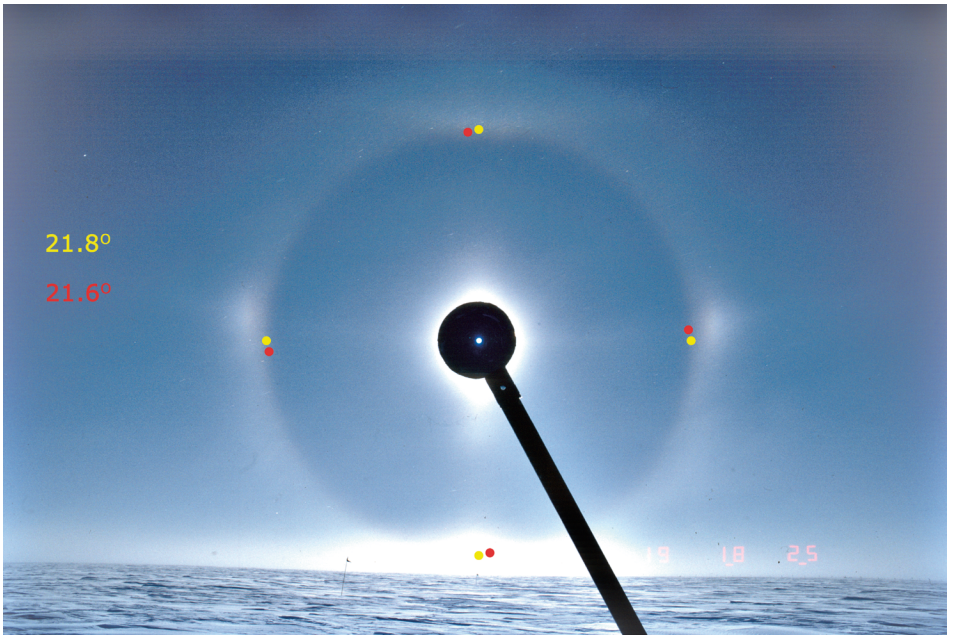

FIGURE 8.13 Another display with 22° halo. South Pole, December 19, 1997.

FIGURE 8.14 Odd radius halos forming in very small crystals. Due to diffraction, the halos are so diffuse that their inner edges are impossible to locate with any precision. The halos here are virtually indistinguishable from each other. Fairbanks, January 19, 1996.

makes the sun look far bigger than its half-degree diameter. We can imagine that those things matter, but we have no idea of their relative importance. Anyway, halos look slightly bigger when they are very bright than when they are dim—bigger in the sense that they expand in all directions. That means that the radius of a circular halo will appear to decrease slightly as the halo brightens.

A light ray that is nearly horizontal can sometimes be bent downward slightly by atmospheric refraction, thus raising the light point of the ray by a few tenths of a degree. A ray that is more oblique to the horizon, however, will be nearly straight. The detailed ramifications of this are beyond us, but we can see that atmospheric refraction might introduce an uncertainty of a few tenths of a degree in a halo radius that has one (but not both) of its endpoints near the horizon. One of the endpoints is of course the sun, the other is on the halo.

Finally, diffraction. When the halo-making crystals are small, diffraction broadens the halos and decreases their apparent radii. The decrease can be substantial. (If the crystals are very small, diffraction will wipe out the halos entirely.) We do not know how to incorporate diffraction rigorously into halo simulations. Luckily, halo displays in which diffraction plays a role are easy to spot, due to their diffuse and poorly defined halos (Figure 8.14). Moreover, although diffraction can decrease halo radii, it cannot increase them; an observed

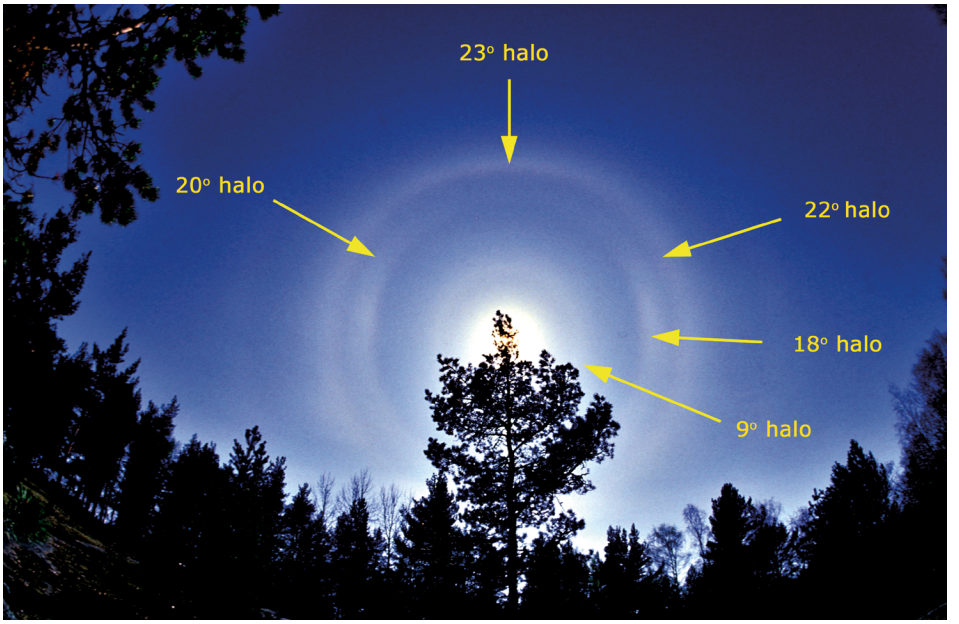

FIGURE 8.15 Odd radius halos. We believe that the halo identifications are correct, but we have not measured the radii. Kustavi, Finland, May 14, 1988. $\Sigma = 44°$. Photo © Pekka Parviainen, Polar Image.

radius that is smaller than $\Delta_{\min}$ can sometimes be attributed to diffraction, but an observed radius that is larger than $\Delta_{\min}$ cannot.

More on the problem of measuring halo radii can be found in an article by Können and Tinbergen [39].

Circular halos are rare

If we insist that circular halos arise in truly random crystal orientations, then circular halos are rare. The halos in the British Columbia display (Figure 8.1) may indeed be circular, but many of the other halos shown in this chapter exhibit intensity variations that are inconsistent with perfectly random orientations. Figures 8.5, 8.15, and 8.16 are examples. Look for weakness or absence of the 18° halo in the 12:00 position, enhancement of the 23° halo in the 12:00 position, or enhancement of the 9° halo in the 6:00 position; these are signs that the crystal orientations have some tendency toward plate orientations rather than being truly random. One can argue about whether the halos in those figures should be called poorly defined plate arcs rather than circular halos. There is no hard and fast line that separates plate arcs (or column arcs) from circular halos. Instead there is a continuum of halos between well-defined plate arcs on one end and truly circular halos on the other.

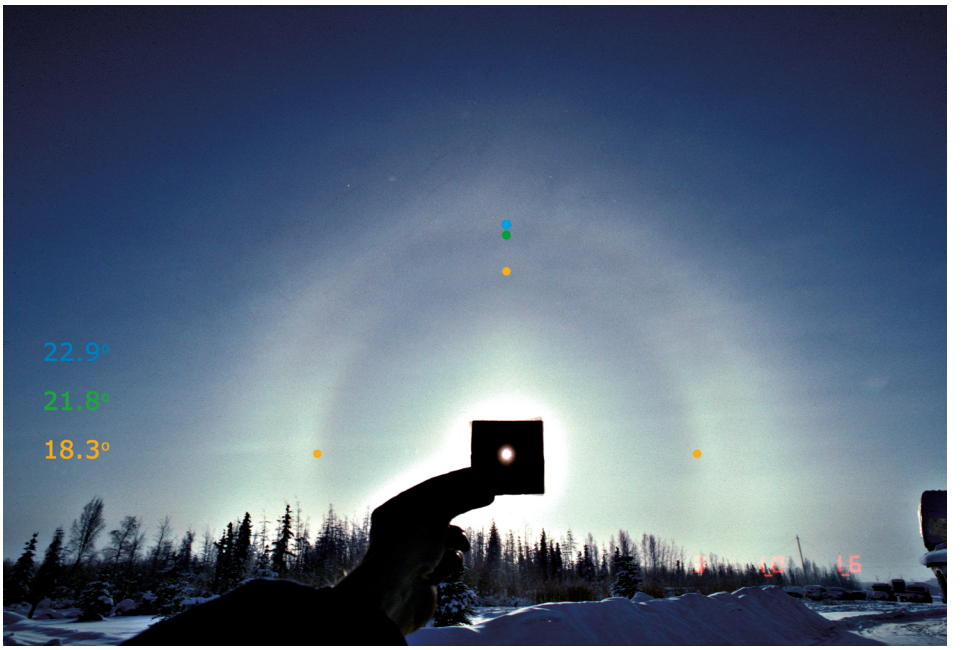

FIGURE 8.16 Odd radius halos, mainly the 18° and 23° halos. The colored dots are positioned at the indicated angular distances from the sun (Table 8.1). Fairbanks, March 3, 1999. Σ = 12°.

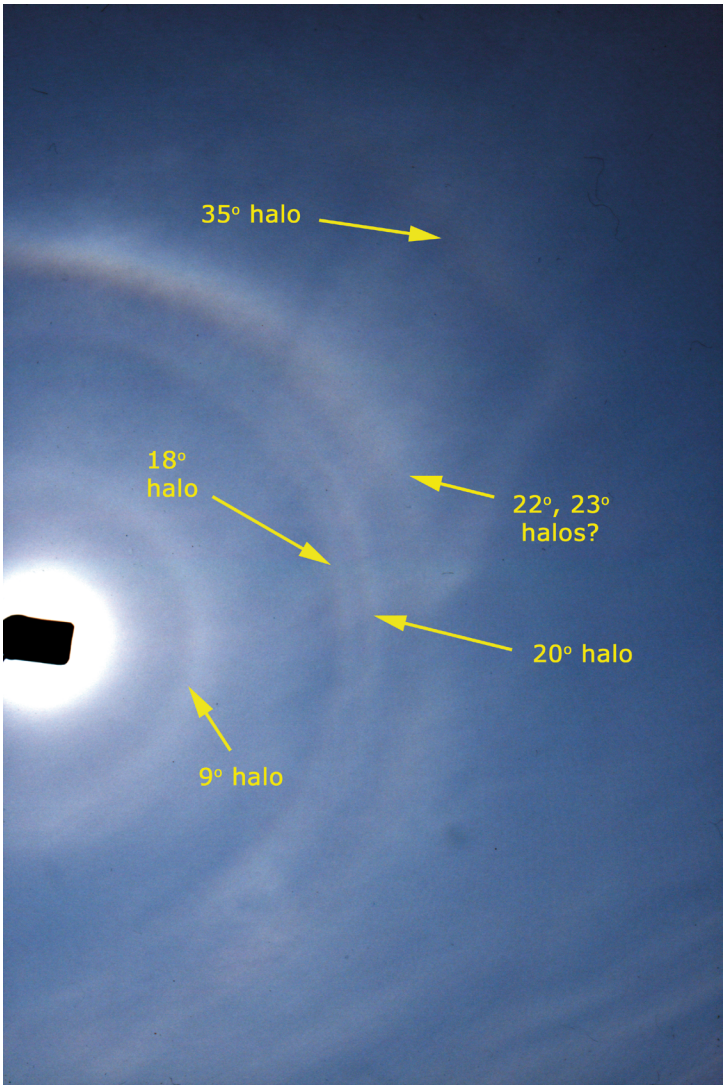

FIGURE 8.17 Odd radius halos, Vaala, Finland, May 13, 2002. For reasons that are not understood, the 20° halo is not common. Here it is unusually bright and distinct. $\Sigma = 44°$.